Chapter III

"Solution Structure of Ca^{2+}/CaM–W-7 Complex: the Basis of Diversity in Molecular Recognition"

III-1 Summary

The solution structure of calcium-bound calmodulin (CaM) complexed with an antagonist, *N*-(6-aminohexyl)-5-chloro-1-naphthalenesulfonamide (W-7), has been determined by multidimensional NMR spectroscopy. The structure consists of one molecule of W-7 binding to each of the two domains of CaM. In each domain, the W-7 chloronaphthalene ring interacts with four methionine methyl groups and other aliphatic or aromatic side-chains in a deep hydrophobic pocket, the site responsible for CaM binding to CaM-dependent enzymes such as myosin light chain kinases (MLCKs) and CaM kinase II. This competitive binding at the same site between W-7 and CaM-dependent enzymes suggests the mechanism by which W-7 inhibits CaM to activate the enzymes. The orientation of the W-7 naphthalene ring in the N-terminal pocket is rotated approximately 40° with respect to that in the C-terminal pocket. The W-7 ring orientation differs significantly from the Trp 800 indole ring of smooth muscle MLCK bound to the C-terminal pocket and the phenothiazine ring of trifluoperazine bound to the N- or C-terminal pocket. These comparative structural analyses demonstrate that the two hydrophobic pockets of CaM can accommodate a variety of bulky aromatic rings, which provides a plausible structural basis for the diversity in CaM-mediated molecular recognition.

III-2 Introduction

CaM antagonists are frequently used to study Ca^{2+}/CaM-dependent activation of various enzymes. In particular, *N*-(6-aminohexyl)-5-chloro-1-naphthalenesulfonamide (W-7) and 10-[3-(4-methylpiperazin-1-yl)propyl]-2-(trifluoromethyl)-10*H*-phenothiazine (trifluoperazine, TFP) have been extensively used for this purpose (Figure III-1). Crystal structures of Ca^{2+}/CaM complexed with TFP have been reported by two groups (Cook *et al.*, 1994, Vandonselaar *et al.*, 1994), but their results differed significantly. In the crystal structure reported by Cook *et al.* (Cook *et al.*, 1994), only one TFP molecule was identified binding to the C-terminal hydrophobic pocket of CaM, while the crystal structure reported by Vandonselaar *et al.* (Vandonselaar *et al.*, 1994) had four TFP molecules: two of them binding to the hydrophobic pocket in each domain of CaM, respectively, and the other two located in the cleft between the CaM domains. Comparisons show that the orientation of the TFP phenothiazine ring binding to the C-terminal hydrophobic pocket of Ca^{2+}/CaM differs by nearly 180° between the two structures. To further complicate matters, a previous NMR study indicated that two TFP molecules bind to one Ca^{2+}/CaM molecule in solution (Craven *et al.*, 1996; Dalgano *et al.*, 1984; Klevit *et al.*, 1981). The stoichiometry of W-7 binding to Ca^{2+}/CaM is also in a similarly complicated situation. Gel filtration experiments reported that three W-7 molecules bind to Ca^{2+}/CaM with a dissociation constant of 11 μM (Hidaka *et al.*, 1979), whereas a recent NMR study on the interaction of the CaM C-terminal half fragment with *N*-(8-aminooctyl)-5-iodo-1-naphthalenesulfonamide (J-8), a derivative of W-7, suggested that one J-8 molecule binds to the C-terminal domain with the terminal amino group of J-8 being highly mobile. However, the position and orientation of the J-8 naphthalene ring in the hydrophobic pocket remains unclear (Craven *et al.*, 1996).

In this chapter, I report the first three-dimensional structure of Ca^{2+}/CaM complexed with W-7, using heteronuclear multidimensional NMR spectroscopy. The binding site and the orientation of W-7 in each domain of Ca^{2+}/CaM have been clearly defined. My present structure provides the first view of Ca^{2+}/CaM recognizing a naphthalenesulfonamide derivative. The structural comparison of this structure with other published structures of CaM-peptide and CaM-ligand complexes helps to reveal the basis of diversity in molecular recognition by Ca^{2+}/CaM.

III-3 Materials and Methods

III-3-1 Sample preparation

W-7 hydrochloride was purchased from Seikagaku Kogyo Co., Ltd. and used without further purification. Uniformly ^{15}N- or $^{15}N/^{13}C$-labeled recombinant *Xenopus laevis* CaM was expressed in *Escherichia coli* and purified to homogeneity as previously described (Ikura *et al.*, 1990a). CaM was dissolved in unbuffered 0.4 ml 95 % H_2O/5 % D_2O or 99.99 % D_2O solution containing 0.1 M KCl and 10.6 mM $CaCl_2$. The pH/pD values of the samples were 6.8 without consideration of the isotope effects. The sample concentrations of CaM were 1.5 mM. The W-7 concentrations of the samples used for three-dimensional structure determination were 7.5 mM.

III-3-2 NMR Spectroscopy

All of the NMR spectra were measured at 35 °C on a Bruker AMX-600 spectrometer, except for where stated. The assignments of W-7 in the absence of Ca^{2+}/CaM were carried out in D_2O solution by 1D-NOE and ^{15}N-^{1}H HMBC experiments on a JEOL JNM-α500 spectrometer. The assignments were transferred to those of W-7 complexed with unlabeled Ca^{2+}/CaM from the titration experiments by 1D ^{1}H, 2D DQF-COSY (Rance *et al.*, 1983), and 2D NOESY. W-7 was also titrated in aliquots of 0.33 protein equiv. into a uniformly $^{13}C/^{15}N$-labeled sample of the protein. After the addition of each aliquot of W-7, 1D ^{1}H, 2D ^{15}N-^{1}H HSQC (Kay *et al.*, 1992; Palmer III *et al.*, 1991), and 2D ^{13}C-^{1}H CT-HSQC (Vuister & Bax, 1992) spectra were acquired. Finally, spectra with 0, 0.33, 0.66, 1.0, 1.33, 1.66, 2.0, 2.5, 3.0, 3.5, 4.0, 5.0, and 6.0 equivalents of W-7 to CaM were recorded. Sequential assignments of the backbone resonances were mainly achieved by a pair of HNCACB (Wittekind & Mueller, 1993) and CBCA(CO)NH (Grzesiek & Bax, 1992a; Szyperski *et al.*, 1994), and further confirmed by another set of experiments,

^{15}N-edited TOCSY-HMQC, HNHA (Vuister & Bax, 1993) and HBHA(CBCACO)NH (Grzesiek & Bax, 1993). Side-chain assignments were obtained from H(CCO)NH (Grzesiek *et al.*, 1993), C(CO)NH (Grzesiek *et al.*, 1993), and HCCH-TOCSY (Bax *et al.*, 1990) experiments. The experimental details are the same as previously reported (Ames *et al.*, 1994). All data were processed using the software nmrPipe and nmrDraw (Delaglio, 1993; Delaglio *et al.*, 1995), and the data analysis was assisted by the software Pipp (Garrett *et al.*, 1991). Slowly exchanging amide protons were identified by monitoring the ^{1}H/D exchange rate of the backbone amides from a series of sensitivity-enhanced ^{15}N-^{1}H HSQC spectra recorded at different time points (7, 22, 52, 112, 202, 292, 382, 472, 592, and 712 min) immediately after dissolving the lyophilized Ca^{2+}/CaM complexed with W-7 in D_2O at 25 °C. The backbone coupling constants, $^{3}J_{HNH\alpha}$, were measured from a HNHA experiment (Vuister & Bax, 1993). Stereospecific assignments of valine and leucine methyl groups were obtained by analyzing ^{13}C-^{1}H HSQC spectrum of 10 % ^{13}C-enriched Ca^{2+}/CaM complexed with W-7 (Neri *et al.*, 1989). Stereospecific assignment of β-methylene groups were carried out by analyzing the NOE patterns of amide and β protons from ^{15}N-edited NOESY-HMQC (Marion *et al.*, 1989), $^{3}J_{H\alpha H\beta}$ from DQF-COSY (Rance *et al.*, 1983), and $^{3}J_{NH\beta}$ from HNHB (Archer *et al.*, 1991). The ^{1}H, ^{13}C, and ^{15}N resonance assignments has been deposited with the BioMagResBank, with accession number of 4056.

III-3-3 Structure Calculation

Approximate interproton distances were obtained from ^{13}C-edited NOESY-HMQC (Ikura *et al.*, 1990b), ^{15}N-edited NOESY-HMQC (Marion *et al.*, 1989), [^{13}C/F_3]-filtered [^{13}C/F_1]-edited HMQC-NOESY (Lee *et al.*, 1994), and a homonuclear 2D NOESY experiments. The mixing time was 100 ms for all

NOESY experiments. Since only one set of W-7 signals was observed, the intermolecular NOEs between Ca^{2+}/CaM and W-7 were assigned either N-terminal or C-terminal complex based on the residue number of CaM. The distance restraints were grouped into three classes: 1.8-2.7, 1.8-3.3 and 1.8-5.0 Å corresponding to strong, medium, and weak NOE cross-peak intensities, respectively. The NOEs including backbone amide protons were grouped into three classes of 1.8-2.9, 1.8-3.5, and 1.8-5.0 Å. ϕ and ψ dihedral angle restraints were derived from the $^3J_{HNH\alpha}$ coupling constants and chemical shift indices (Wishart & Sykes, 1994). Values of -60° ± 30° and -40° ± 30° were used for ϕ and ψ dihedral angles, respectively, for α-helical regions; -120° ± 50° and 120° ± 50° for β-strands. Hydrogen bond restraints were obtained by analyzing the ^{1}H/D exchange rates and the NOE patterns characteristic of α-helices or β-strands. Two distance restraints, $r_{NH\text{-}O}$(0-2.3 Å) and $r_{N\text{-}O}$(0-3.3 Å), were used for each hydrogen bond. Structures were calculated using the YASAP protocol (Nilges *et al.*, 1988) within X-PLOR (Brünger, 1992) as previously described (Bagby *et al.*, 1994). The final structures were calculated based on 2111 interproton distance restraints (781 intraresidue, 500 sequential, 432 short-range, 301 long-range, 97 intermolecular), 114 distance restraints for hydrogen bonds, 24 distance restraints for four Ca^{2+} coordinations, and 211 dihedral angle restraints. The coordinates for the final structures and structural constraints used in the calculations have been deposited with the Protein Data Bank, Chemistry Department, Brookhaven National Laboratory, NY 11973 USA, with accession code of 1MUX. In this chapter, color figures except for Figure III-6c and Figure III-7c were generated using Insight II (Biosym, San Diego, CA).

III-4 Results and Discussion

III-4-1 NMR Spectral Changes and Stoichiometry

Given the considerable disagreements in the literature concerning the number of antagonist molecules which bind to a molecule of CaM, I monitored changes in the 1D and NOESY spectra upon addition of W-7 to unlabeled CaM, and in the ^{15}N-^{1}H HSQC and ^{13}C-^{1}H CT-HSQC spectra upon addition of unlabeled W-7 to uniformly $^{13}C/^{15}N$ labeled CaM. W-7 was titrated up to six equivalents of Ca^{2+}/CaM, during which the W-7 signals were gradually shifted and only one set of W-7 signals was observed. Most of the HSQC peaks of CaM were also gradually shifted with little changes in their intensities. These results suggest that exchanges between W-7 bound state and unbound state are fast on the NMR time scale. Most of the spectral change occurs from zero to two equivalents of Ca^{2+}/CaM, but smaller changes in chemical shift are observed for some peaks upon addition to six equivalents. A similar phenomenon was also reported for Ca^{2+}/CaM complexed with J-8 (Craven *et al.*, 1996), a derivative of W-7. The most notable changes are seen in the methionine methyl region of ^{13}C-^{1}H CT-HSQC spectra (Figure III-2). All methionine methyl groups except for Met 76 showed drastic high-field shifts, presumably due to ring current effects caused by the direct contact with the W-7 aromatic ring. Similar high-field shifts of a few methionine methyl groups have also been reported in Ca^{2+}/CaM complexed with TFP (Klevit *et al.*, 1981, Dalgano *et al.*, 1984) and with peptides (Siivari *et al.*, 1995; Zhang & Vogel, 1994). The importance of the methionine will be discussed later.

All the methionine methyl groups with high-field shifts upon W-7 binding have NOEs with the W-7 naphthalene ring and are located in the hydrophobic pocket. Another intermolecular NOEs observed for the naphthalene were all with the residues in the hydrophobic pocket in each Ca^{2+}/CaM domain. The titration and intermolecular NOE data strongly suggest that one W-7 molecule binds to each Ca^{2+}/CaM domain with high

affinity. Since the intermolecular NOE patterns did not change after the addition of more than two equivalents of W-7 to Ca^{2+}/CaM, the third possible binding site must have much lower affinity with W-7 than the other two sites and was not detected in this NMR analysis. Five W-7 molecules per Ca^{2+}/CaM are enough to saturate the two binding site of high affinity (Figure III-2), and this condition was selected for the structure determination. The resulting structures of Ca^{2+}/CaM with two W-7 molecules were completely consistent with the NMR-derived constraints obtained for the experimental conditions.

III-4-2 The Structure of Ca^{2+}/CaM Complexed with W-7

The three-dimensional structure of Ca^{2+}/CaM complexed with W-7 has been determined using 2436 experimental restraints, including 97 intermolecular distance restraints derived from NMR spectroscopy. Due to the lack of NOEs between the N and C-terminal domains, it is impossible to superimpose both domains of the 30 NMR-derived structures simultaneously. Hence, I present the structures of the two domains separately. Figure III-3a shows the best-fit superposition of the backbone atoms of the N- and C-terminal domains. Structural statistics are summarized in Table III-1.

The backbone conformation of each Ca^{2+}/CaM domain remains essentially unchanged upon complexation with W-7 (Figure III-3b). The chloronaphthalene group of W-7 binds to the hydrophobic pocket of each domain of Ca^{2+}/CaM, with the chlorine atom pointing towards the bottom of the pocket (Figure III-3). No intermolecular NOE was observed for the terminal two methylene groups of W-7, suggesting that the methylene groups are not involved in specific Ca^{2+}/CaM interactions. Thus, the complex is mainly stabilized by the van der Waals interactions between the hydrophobic side-chains of Ca^{2+}/CaM and the chloronaphthalene group of W-7.

Orientation of the bound W-7 molecule is generally similar in both the N and C-terminal domains (Figure III-4). This result was anticipated as the N and C-terminal domains are homologous (44 % residue identity). Especially, the set of hydrophobic side-chains responsible for interactions with W-7 are extremely similar between the two domains: Phe 19/Phe 92, Ile 27/Ile 100, Leu 32/Leu 105, Met 36/Met 109, Met 51/Met 124, Ile 52/Ile 125, Val 55/Ala 128, Ile 63/Val 136, Phe 68/Phe141, Met 71/Met 144, and Met 72/Met 145 respectively in the N/C-terminal domain. A difference has been found in the orientation of the naphthalene rings which are rotated by approximately 40° relative to one another (Figure III-3b). This may be due to the amino acid replacements of Val 55 to Ala 128 and of Ile 63 to Val 136, as side-chains in the N-terminal domain are more bulky.

The naphthalene ring of W-7 is sandwiched between two hydrophobic walls (Figure III-4). One consists of Phe 68/Phe 141, Met 71/Met 144, and Met 72/Met 145 side-chains, and the other uses Leu 32/Leu 105, Met 36/Met 109, and Met 51/Met 124 side-chains. These two walls are also flanked by Val 55/Ala 128 and Phe 19/Phe 92 (Figures III-4, III-6a). The orientation of W-7 in the pocket seems to be determined by the position of the chlorine atom on the naphthalene ring as I observe the chlorine atom located in the deepest part of the hydrophobic pocket of both domains.

A series of W-7 derivatives in which the chlorine atom was substituted to H, F, Br, and I (herein referred to as W-7(H), W-7(F), W-7(Br), and W-7(I), respectively) have been functionally tested (MacNeil *et al.*, 1988; Tanaka *et al.*, 1982). Their 50 % inhibitory concentrations, IC_{50}, for Ca^{2+}/CaM dependent activation of phosphodiesterase were 240 μM for W-7(H), 50 μM for W-7(F), 31 μM for W-7, 25 μM for W-7(Br), and 29 μM for W-7(I). In Figure III-5, their IC_{50} values are plotted versus the van der Waals radius and the electronegativity of these substituted atoms. The extent of inhibition correlates better with the van der Waals radius than electronegativity,

suggesting that van der Waals contacts are the dominant force contributing to the difference in inhibitory activity. To this end, it is relevant to note that the W-7 binding pockets of both N and C-terminal domains are completely hydrophobic and possess no polar or charged group. These side-chains, which form the pocket undergo significant rearrangements upon complexation, and as I shall discuss later, this appears to be a general mechanism in Ca^{2+}/CaM molecular recognition.

III-4-3 Comparison of W-7 and Target Peptide Bound to Ca^{2+}/CaM

Ca^{2+}/CaM can bind to numerous target proteins (James *et al.*, 1995; Means *et al.*, 1991; Vogel, 1994). In the structures of Ca^{2+}/CaM complexed with different target peptides (Ikura *et al.*, 1992; Meador *et al.*, 1992; Meador *et al.*, 1993), a bulky hydrophobic residue binds to the hydrophobic pocket corresponding to the W-7 binding site: Leu 813/Trp 800 in smMLCK, Phe 593/Trp 580 in skMLCK, and Leu 308/Leu 299 in CaMKII. I compare the binding mode of tryptophan to that of W-7, since only tryptophan is inserted into the deepest part of the pocket among the reported structural complexes.

Figures III-6a and b show surface representations of the C-terminal hydrophobic pocket bound to W-7 and the smMLCK Trp 800 (Meador *et al.*, 1992), respectively. In the latter Trp 800 anchors the peptide to the hydrophobic pocket with its 6-membered ring at the bottom of the pocket and the 5-membered ring near the exit (Figures III-6b, c). The deep insertion of the Trp 800 indole ring is assisted by the Cβ atom acting as a spacer between the aromatic ring and the peptide backbone. The indole ring leans towards the Ala 128 side of the binding pocket, and is stabilized by a hydrogen bond between NεH of Trp 800 and the carbonyl oxygen of Met 124 of Ca^{2+}/CaM. In contrast, the naphthalene ring of the W-7 sits in the middle of the binding pocket and its

sulfonamide group, which is in a similar location to the Cβ of Trp 800, is too bulky to enter the hydrophobic pocket.

The conformations of most of the side-chains interacting directly with Trp 800, such as Ile 100, Leu 105, Met 124, Ile 125, Ala 128, Val 136, and Met 144 are almost the same as those in the W-7 complex. Although the chemical structures of tryptophan and W-7 differ significantly, superpositions show that most of the indole van der Waals surface of Trp 800 overlaps with the chlorine containing ring of W-7. Thus, CaM can recognize these slightly different shapes without changing its own conformation. On the other hand, the other W-7 ring contacts the Phe 92 side of the pocket, suggesting that a chloronaphthalene ring is the maximum size which can be accommodated in the hydrophobic pocket. Phe 92, Met 109, and Met 145 side-chains have van der Waals contacts with W-7, although they don't have contacts with Trp 800. Structural rearrangements are observed in the methyl groups of Met 109 and Met 145 which change their positions to interact with the W-7 aromatic ring.

Clearly, W-7 molecules completely shield the key hydrophobic site in each CaM domain. Both sites are crucial for binding of target proteins such as MLCKs (Ikura *et al.*, 1992; Meador *et al.*, 1992) and CaMKII (Meador *et al.*, 1993). The dissociation constant of a target peptide for CaM is, however, significantly lower (~10^{-9} M in the case of MLCK peptide M13) than that of W-7. The difference can be accounted for by two factors: (1) the CaM binding region in target proteins is composed of a single polypeptide chain that interacts simultaneously with the two hydrophobic sites of CaM, (2) other hydrophobic and basic groups in the CaM binding region of target proteins provide additional binding energy.

III-4-4 Comparison of the Ca^{2+}/CaM Binding Mode between W-7 and TFP

Two previously reported structures of Ca^{2+}/CaM complexed with TFP have been compared with the present structure. It is important to note that the phenothiazine ring orientation of the C-terminal Ca^{2+}/CaM domain reported by Vandonselaar *et al.* (Vandonselaar *et al.*, 1994) differs from that by Cook *et al.* (Cook *et al.*, 1994) with the ring rotated by approximately 180° along the middle phenothiazine ring (Figures III-7a and b). Figure III-7c shows a schematic drawing of W-7 (this study) and TFP (Cook *et al.*) bound to the C-terminal hydrophobic pocket. Interestingly, there is no close correspondence between any of the ring systems of W-7 and TFP, since TFP has a large phenothiazine ring with a trifluoromethyl group attached to one side, which is too large to enter the pocket completely. Therefore, only one side of tricyclic TFP ring can be inserted into the pocket, leaving the other side of the ring out of the pocket.

The TFP phenothiazine ring has van der Waals contacts with the pocket as expected. The conformations of all side-chains interacting with TFP such as Ile 100, Leu 105, Met 124, Ile 125, Ala 128, Val 136, and Met 144 are quite similar to those in W-7 complex. However, other residues forming the pocket such as Phe 92, Met 109, Phe 141, and Met 145 do not interact with TFP directly, even though van der Waals contacts were observed with the W-7 complex. As a consequence, the conformations of some of these residues, in particular Met 109 and Met 145, change significantly when interacting with W-7.

Aside from interactions with the hydrophobic pocket, the TFP piperazine ring, which is outside the pocket, also has close contacts with M144. This may cause the phenothiazine ring to bind to the Ala 128 side of the pocket. Both interactions of phenothiazine within the pocket and the piperazine outside the pocket appear to contribute to the stabilization of the

complex in the crystal. In W-7, it is only the chloronaphthalene ring which has specific interactions with the inside of the pocket, although I also observe a few intermolecular NOEs between its methylene protons and Ca^{2+}/CaM. These NOEs enable me to roughly determine the locations of the methylene groups near the binding pocket, which is quite different from that of TFP.

III-4-5 Fine Tuning in CaM Conformation

As described above, the backbone conformation of each domain of Ca^{2+}/CaM remains essentially unchanged upon binding to W-7 (Figure III-3b). This is also the case when Ca^{2+}/CaM binds to target peptides (Ikura *et al.*, 1992; Meador *et al.*, 1992; Meador *et al.*, 1993; Roth *et al.*, 1992). Then how does CaM adapt its conformation in order to optimize interaction with a particular target molecule? This is most likely achieved by a fine adjustment of side-chain conformations mainly involving eight out of CaM's nine methionines (excluding Met 76).

^{13}C-^{1}H CT-HSQC spectra of Ca^{2+}/CaM upon addition of W-7 (Figure III-2) clearly illustrate the significance of methionine residues in the complex formation. The ^{1}H chemical shift differences of CaM methyl groups between free Ca^{2+}/CaM and Ca^{2+}/CaM complexed with W-7 (Figure III-8a), show that most notable changes upon W-7 binding are for the methionine methyl groups; Met 36/Met 109, Met 51/Met 124, Met 71/Met 144, and Met 72/Met 145. In the complex with W-7, these residues form the hydrophobic walls which enclose the chloronaphthalene group of W-7, suggesting that the observed high-field shifts of these methyl groups are due to the ring current effects caused by direct contacts with the naphthalene ring.

Van der Waals interactions between W-7 and CaM side-chains seem to be enhanced by conformational changes in the side-chains. Figures III-8b and c show the side-chains interacting with W-7 in the complex as well as the

corresponding side-chains in the free Ca^{2+}/CaM structure (Chattopadhyaya *et al.*, 1992). A Cα superposition illustrates that side-chain conformations of Phe 19/Phe 92, Met 36/Met 109, Met 51/Met 124, Met 71/Met 144, and Met 72/Met 145 undergo significant changes upon W-7 complexation. The aromatic rings of Phe 19/Phe 92 appear to play a key role in defining the size of the W-7 binding pocket. Positional changes in the Phe 19/Phe 92 aromatic rings facilitate accommodation of the bulky naphthalene ring of W-7 in the pocket. In detail I note a -48.7° ± 6.9°/-22.6° ± 6.2° change in χ_1 and a 48.2° ± 7.2°/44.6° ± 18.3° change in χ_2, respectively.

Methyl groups of methionine side-chain also interact directly with W-7 naphthalene rings by changing their locations. When ligands such as tryptophan and TFP bind to the pocket of the C-terminal Ca^{2+}/CaM domain, only Met 124 and Met 144 interact directly with ligand's aromatic rings. However, in W-7, the naphthalene ring also interacts with Met 109 and Met 145, due to side-chain rearrangements in the latter (Figures III-6a and b, Figures III-7a and b). In general, methionine side-chains are very flexible due to an unbranched side-chain and a long C-S bond, which enables essentially free rotation about the χ_3 torsion angle. This χ_3 flexibility is reflected by the absence of preferred rotamers, usually seen for other side-chains (Gellman, 1991). In addition, sulfur has a larger polarizability than carbon, providing greater van der Waals interactions to occur (Gellman, 1991; Zhang *et al.*, 1994). Due to both the enhanced flexibility and van der Waals effect, methionine side-chains seem highly suited to providing close interactions with bound ligand.

Each hydrophobic pocket of Ca^{2+}/CaM has four methionine residues which occupy in total 46 % of the exposed hydrophobic pocket (O'Neil & DeGrado, 1990). Therefore, fine tuning of these four methionine conformations in each domain, together with Phe 19/Phe 92 in the case of W-

7, might play an essential role in the diversity of molecules recognized by Ca^{2+}/CaM. It should be noted that a different set of methionine and other hydrophobic side-chains may be selected for a different interacting molecule. The importance of methionine side-chains is also supported by recent mutagenesis studies, in which the substitution of methionine to glutamine or leucine in CaM impair the activation of smMLCK, CaMKII, CaMKIV, nitric oxide synthase, and cyclic nucleotide phosphodiesterase (Chin & Means, 1996; George *et al.*, 1996; Zhang *et al.*, 1994). It is noted that even leucine, a similarly hydrophobic but less flexible and polarizable residue than methionine, is unable to take the place of methionine.

III-5 Concluding Remarks

The present structure determination of Ca^{2+}/CaM complexed with W-7, and its comparison with the previously reported structures of Ca^{2+}/CaM complexed with the MLCK peptide and with TFP, have revealed several structural features relevant to the interaction of the hydrophobic pocket of each Ca^{2+}/CaM domain with target peptide and antagonists. W-7 appears to inhibit the CaM-mediated activation of target proteins by blocking the hydrophobic pocket of each domain that normally plays a role in anchoring targets. However, the orientation of the W-7 chloronaphthalene ring in the CaM hydrophobic pocket differs significantly from that of the key tryptophan residue of the MLCK peptide or the phenothiazine ring of TFP. The rearrangements of side-chains such as Phe 19/Phe 92, Met 36/Met 109, and Met 72/Met 145 upon W-7 binding maximize van der Waals contacts with W-7. This fine tuning appears to be a general mechanism for the CaM hydrophobic binding pockets to accommodate various bulky aromatic rings, and thereby provides a plausible structural basis for diversity in target recognition by CaM.

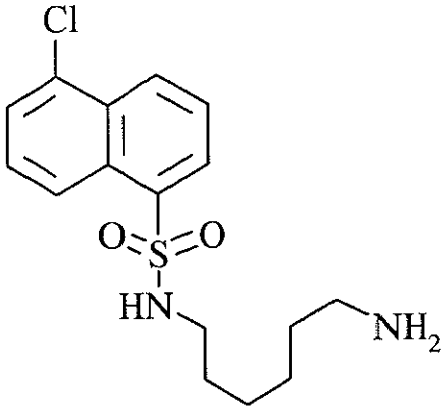

W-7

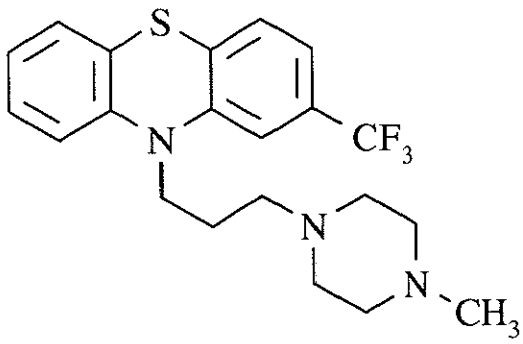

TFP

Figure III-1. Structures of W-7 and TFP.

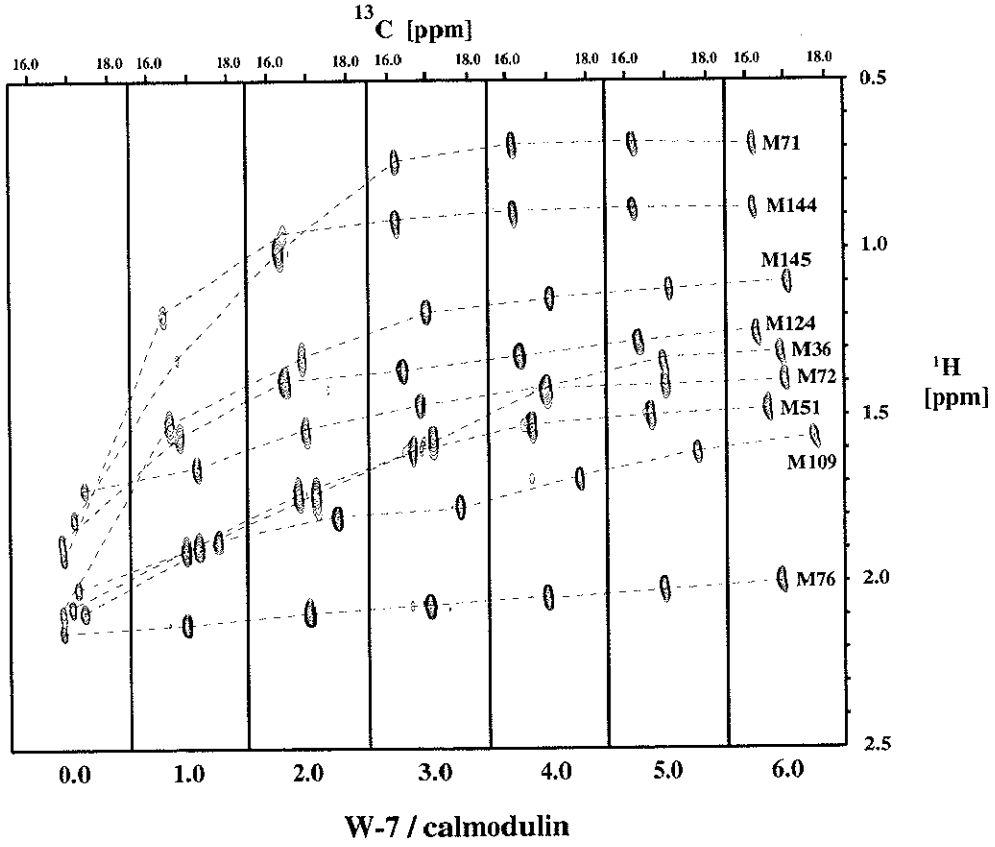

Figure III–2. The ^{13}C–^{1}H HSQC spectra of CaM methionine methyl region at various equivalents of added W–7.

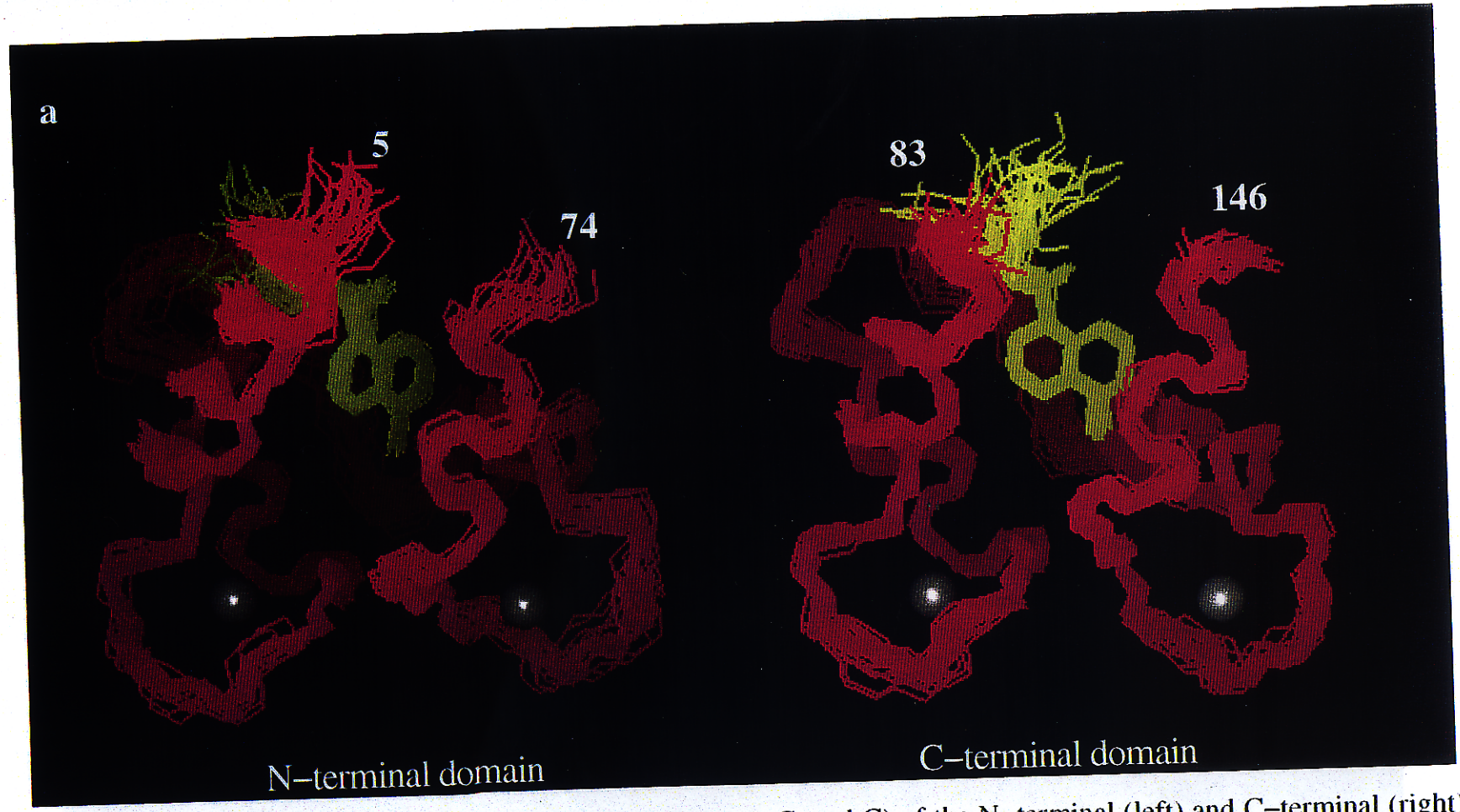

Figure III–3. a, Best–fit superpositions of the backbone atoms (N, C, and C) of the N–terminal (left) and C–terminal (right) domain (magenta) with non–hydrogen atoms of W–7 (yellow) of the selected 30 NMR–derived structures of Ca^{2+}/CaM complexed with W–7. On the left, 30 main–chain structures for the N–terminal domain (residues 5–74) are superimposed onto the energy–minimized average structure using the residues from the regions of regular secondary structure (residues 6–18, 26–39, 45–55, 62–74). These give a R.M.S. deviation of 0.60 ± 0.13 Å for the backbone atoms and 1.24 ± 0.11 Å for all heavy atoms. On the right, the same procedure is shown for the C–terminal domain (residues 83–146). Superposition using regions of regular secondary structure (residues 83–91, 99–111, 118–127, 135–146) yield a R.M.S. deviation of 0.52 ± 0.07 Å for the backbone atoms and 1.24 ± 0.08 Å for all heavy atoms. The residue numbers of N and C termini of each domain are indicated.

Figure III–3. b, Ribbon drawing of the backbone atoms of N–terminal (left, magenta) and C–terminal (right, magenta) domain of the energy–minimized average structure superimposed on the corresponding domain of the crystal structure of Ca^{2+}/CaM (white, Chattopadhaya *et al.*, 1992). W–7 molecules and Ca^{2+} ions are shown in yellow stick models and white balls, respectively. R.M.S. deviations for backbone atoms of the N–terminal domain (residues 6–74) and C–terminal domain (residues 83–146) are 1.17 Å and 1.25 Å, respectively.

Table III-1. Structural statistics of the 30 structures of Ca^{2+}/CaM complexed with W-7[1]

R.M.S. deviations from experimental distance restraints (Å)	
All (2225)	0.020 ± 0.000
Interresidue sequential NOE ($\|i - j\| = 1$) (500)	0.014 ± 0.000
Interresidue short range NOE ($1 < \|i - j\| \leq 5$) (432)	0.017 ± 0.004
Interresidue long range NOE ($\|i - j\| > 5$) (301)	0.020 ± 0.001
Intraresidue NOE (781)	0.014 ± 0.009
Intermolecular NOE (97)[2]	0.040 ± 0.003
Hydrogen bond (114)	0.044 ± 0.009
R.M.S. deviations from experimental dihedral restraints (deg) (211)	0.17 ± 0.06
R.M.S. deviations from idealized geometry	
Bonds (Å)	0.009 ± 0.000
Angles (deg)	1.89 ± 0.00
Impropers (deg)	1.03 ± 0.00
Energies (kcal mol^{-1})	
F_{NOE}[3]	44.65 ± 8.24
F_{cdih}[3]	0.438 ± 0.287
F_{repel}[4]	35.7 ± 6.0
F_{L-J}[5]	-474.4 ± 22.8

[1]The number of each type of restraints used in the structure calculation is given in parenthesis.
None of the structures exhibits distance violations greater than 0.3 Å or dihedral angle violations greater than 1.0°.
[2]36 and 37 NOEs were assigned between the naphthalene ring of W-7 and the N-terminal and C-terminal domains of Ca^{2+}/CaM, respectively, while 12 NOEs between the W-7 methylene groups and each of the N-terminal and C-terminal domain, respectively.
[3]F_{NOE} and F_{cdih} were calculated using force constraints of 50 kcal mol^{-1} $Å^{-2}$ and 200 kcal mol^{-1} rad^{-2}, respectively.
[4]F_{repel} was calculated using a final value of 4.0 kcal mol^{-1} $Å^{-4}$ with the van der Waals hard sphere radii set to 0.75 times those in the parameter set PARALLHSA supplied with X-PLOR (Brünger, 1992).
[5]E_{L-J} is the Lennard-Jones van der Waals energy calculated with the CHARMM empirical energy function and is not included in the target function for simulated annealing calculation.

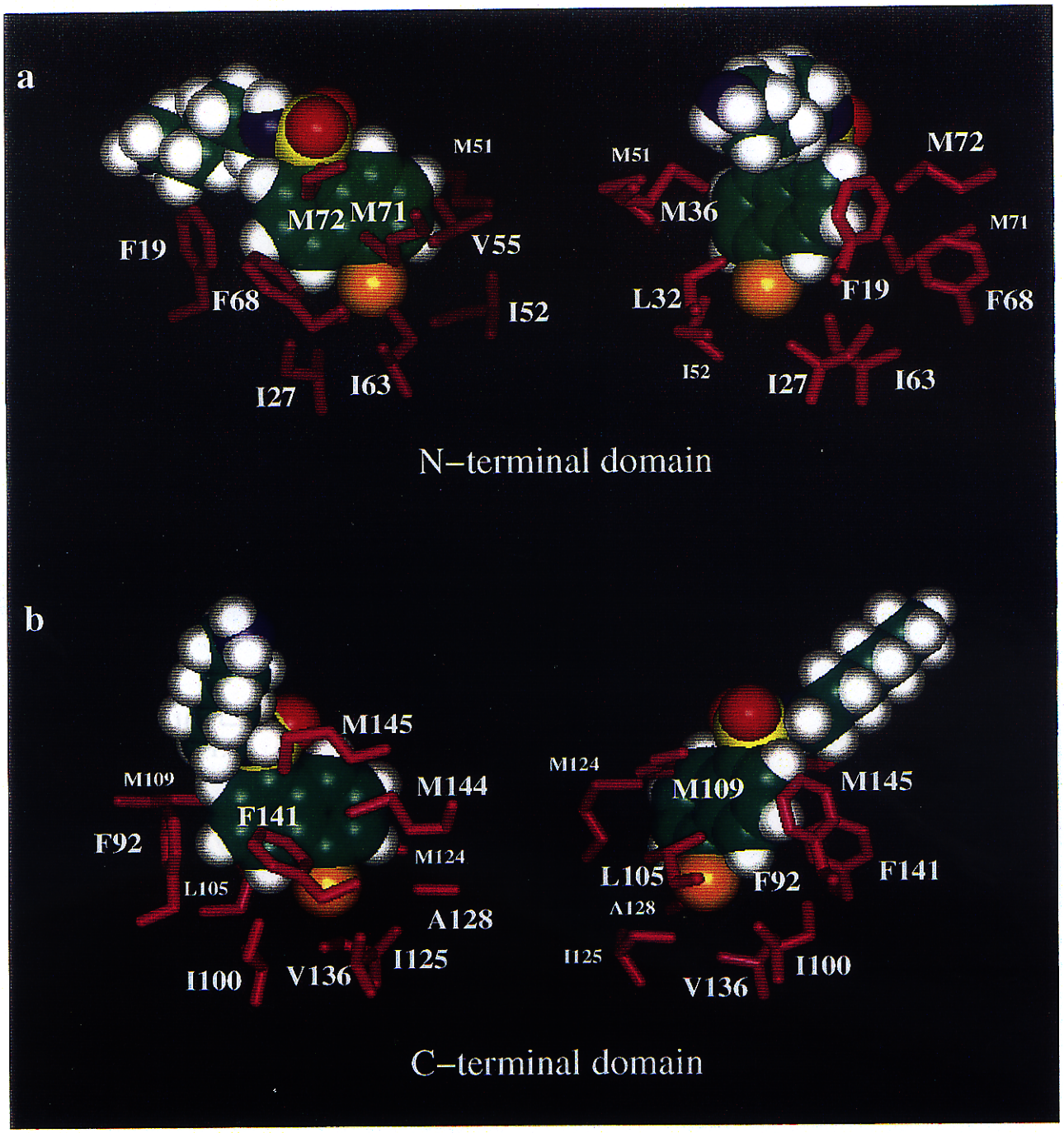

Figure III–4. W–7 binding site in the a, N–terminal and b, C–terminal domain (left, front view; right, side view). W–7 is shown as a space filling model with chlorine in orange, sulfur in yellow, oxygen in red, nitrogen in blue, carbon in green, and hydrogen in white. Hydrophobic side–chains within 5 Å of W–7 are shown in magenta and labeled with a sequence–specific assignment. The structure of terminal methylene and amino groups are arbitrary due to the high flexibility.

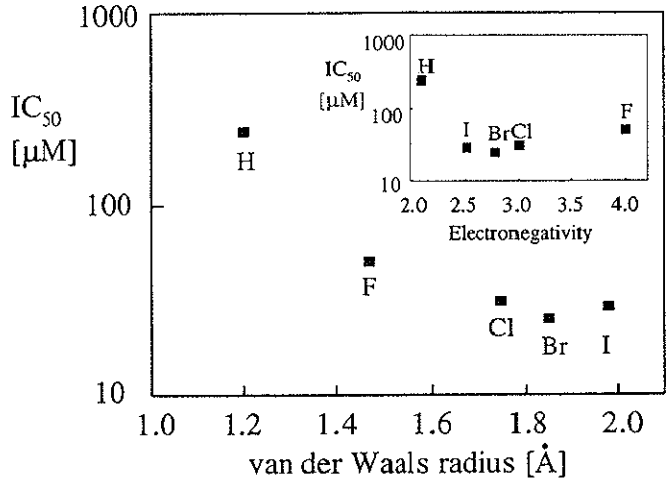

Figure III-5. Fifty percent inhibitory concentrations (IC_{50}) for Ca^{2+}/CaM dependent activation of phosphodiesterase by W-7 derivatives containing a different substituent atom at position 5: W-7(H), W-7(F), W-7, W-7(Br), and W-7(I) (Tanaka *et al.*, 1982; MacNeil *et al.*, 1988). IC_{50} is plotted against van der Waals radius and electronegativity (inset) for halogen atoms and hydrogen.

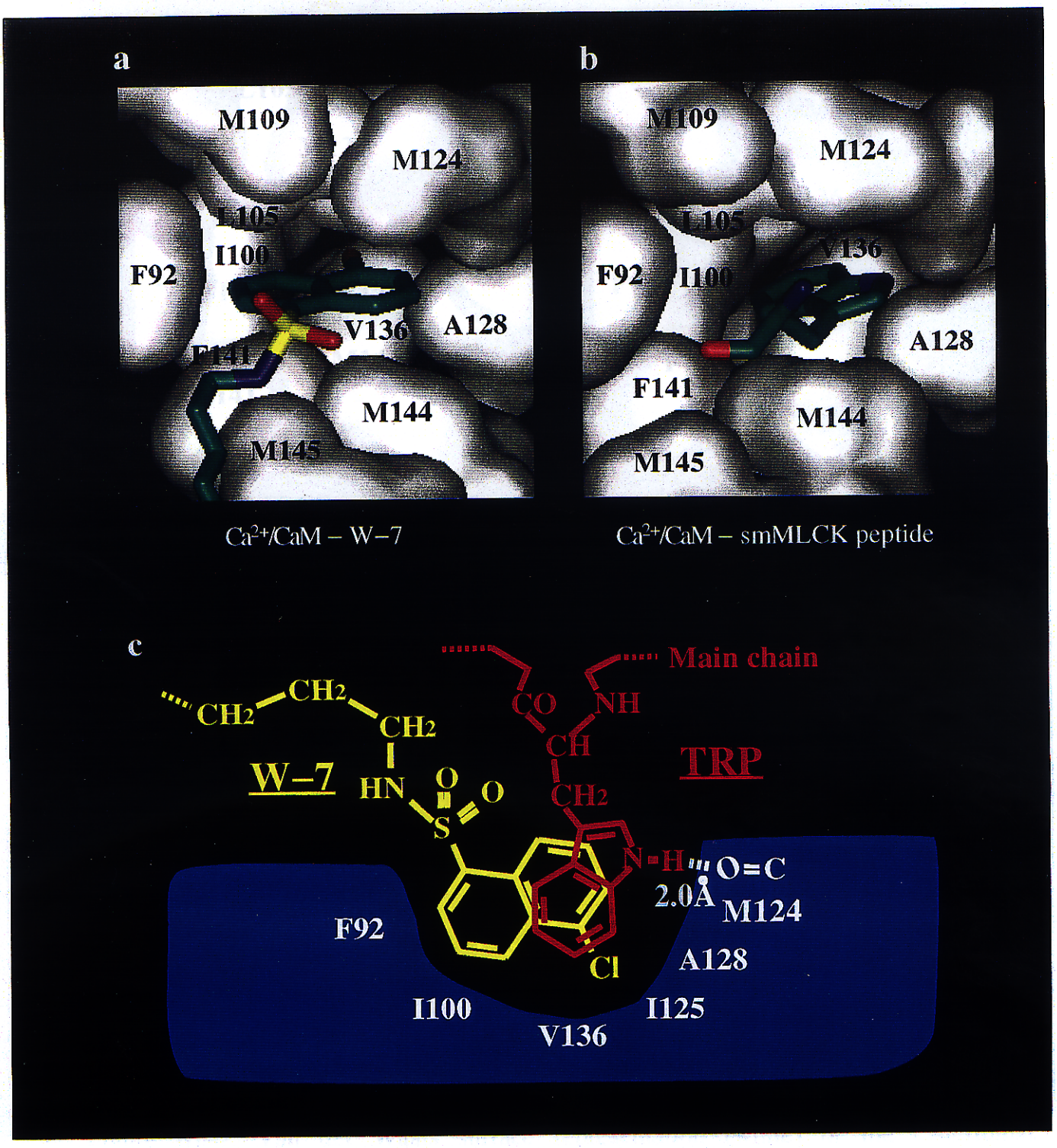

Figure III–6. Van der Waals surface representation (white) of the C–terminal hydrophobic pocket bound to a, W–7 and b, Trp 800 from the smMLCK peptide (Meador *et al.*, 1992). Non–hydrogen atoms of W–7 and Trp 800 are shown as sticks with chlorine in orange, sulfur in yellow, oxygen in red, nitrogen in blue, and carbon in green. Surfaces were generated using SURFNET (Laskowski, 1995). c, Schematic drawing of the C–terminal binding pocket illustrating the differences in orientation between W–7 and smMLCK Trp 800.

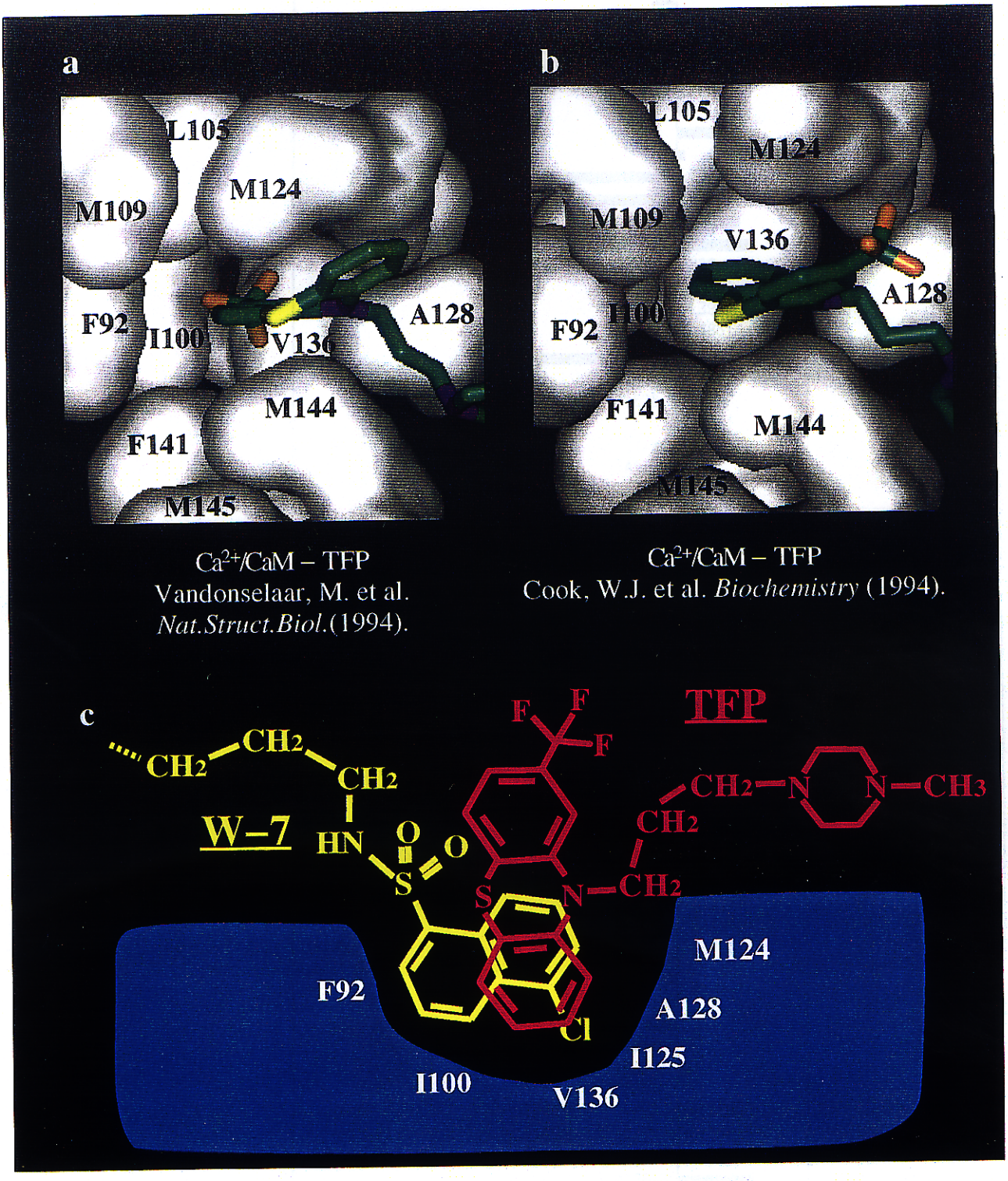

Figure III–7. Van der Waals surface representation (white) of the C–terminal hydrophobic pocket bound to TFP in the structure reported by a, Cook *et al.* (Cook *et al.*, 1994) and b, Vandonselaar *et al.*(Vandonselaar *et al.*, 1994). Non–hydrogen atoms of TFP are shown as stick models with sulfur in yellow, fluorine in orange, nitrogen in blue, and carbon in green. c, Schematic drawing of the C–terminal binding pocket illustrating the differences in orientation between W–7 and TFP (Cook *et al.*, 1994). To compare the recognition of aromatic groups by the hydrophobic pocket of Ca^{2+}/CaM, we use the structure of TFP complex reported by Cook *et al.* (Cook *et al.*, 1994), in which the phenyl ring with no substitution is located at the bottom of the pocket.

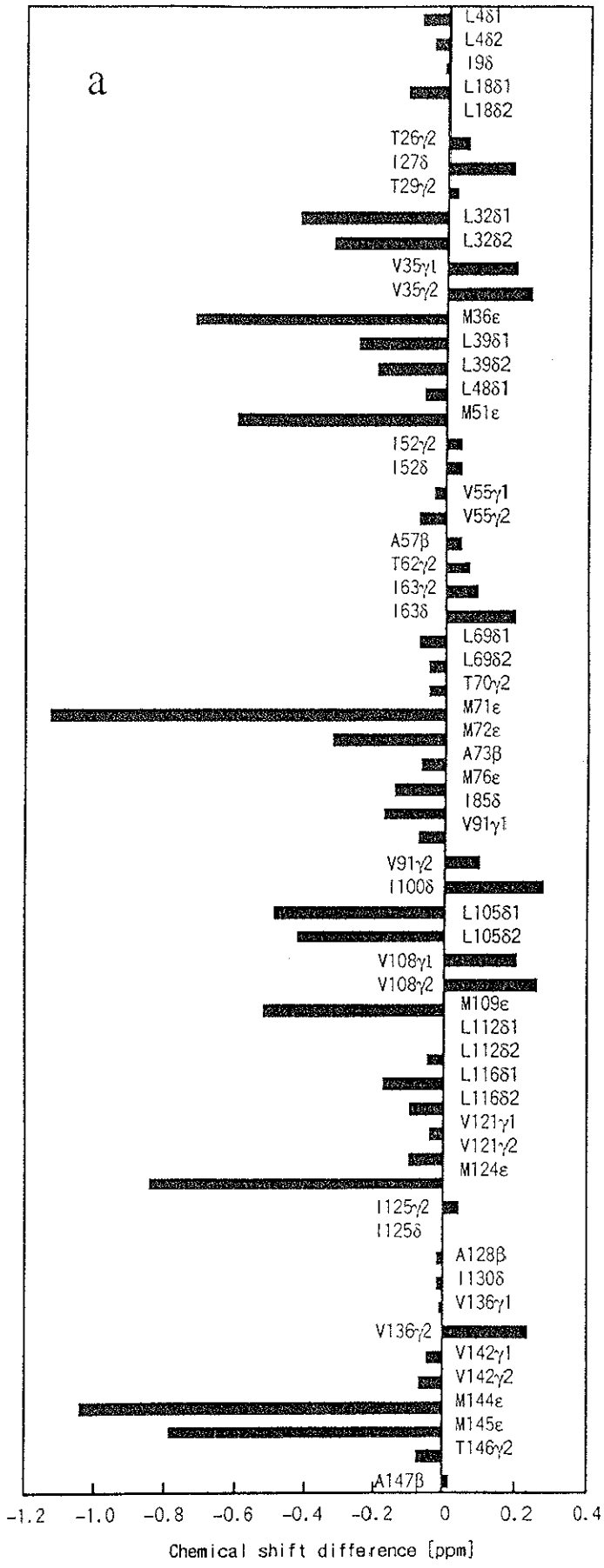

Figure III-8. a, ^{1}H chemical shift changes for Ca^{2+}/CaM methyl groups binding to W-7.

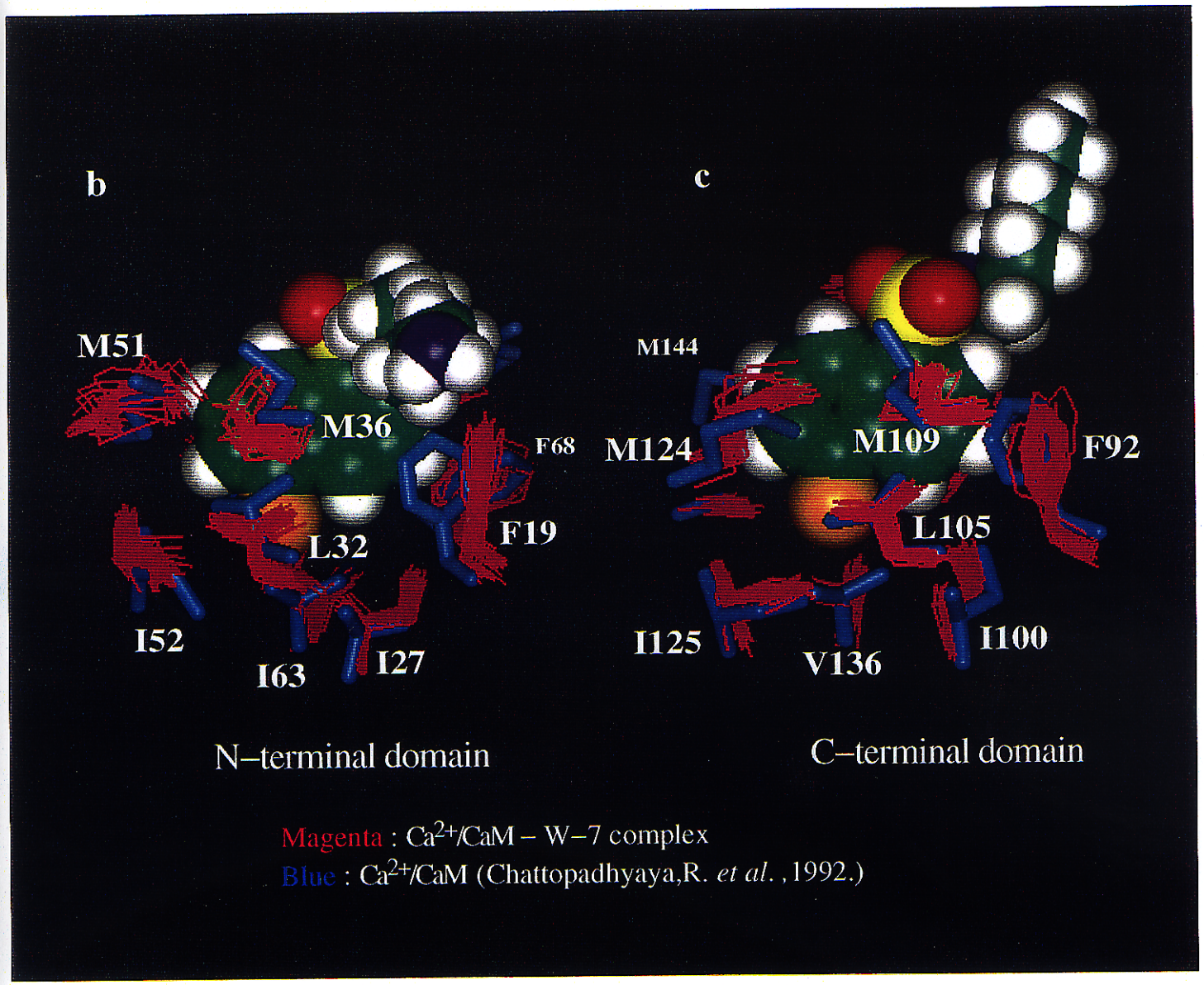

Figure III–8. b, W–7 binding site in the N–terminal domain and c, W–7 binding site in the C–terminal domain of Ca^{2+}/CaM complexed with W–7 and Ca^{2+}/CaM (Chattopadhyaya *et al.*, 1992). The Cα carbon atoms are superimposed. Hydrophobic side–chains of Ca^{2+}/CaM–W–7 complex within 5 Å of W–7 are shown in magenta, and corresponding side–chains of Ca^{2+}/CaM are shown as blue sticks. W–7 is shown as a space filling model with chlorine in orange, sulfur in yellow, oxygen in red, nitrogen in blue, carbon in green, and hydrogen in white.